PHYSICAL REVIEW B **66**, 132417 (2002)

Magnetic structure of antiferromagnetic $NdRhIn_5$

S. Chang,[1,2,*] P. G. Pagliuso,[1,3] W. Bao,[1] J. S. Gardner,[4] I. P. Swainson,[4] J. L. Sarrao,[1] and H. Nakotte[2]
[1]*Los Alamos National Laboratory, Los Alamos, New Mexico 87545*
[2]*Physics Department, New Mexico State University, Las Cruces, New Mexico 88003*
[3]*DEQ-IFGW-UNICAMP, Cidade Universitaria-Barao, Geraldo 13083-970 Campinas-SP, Brazil*
[4]*NRC Canada, NPMR, Chalk River Laboratories, Chalk River, Ontario, Canada K0J 1J0*
(Received 10 May 2002; published 30 October 2002)

The magnetic structure of antiferromagnetic $NdRhIn_5$ has been determined using neutron diffraction. It has a commensurate antiferromagnetic structure with a magnetic wave vector $(\frac{1}{2}0\frac{1}{2})$ below $T_N=11$ K. The staggered Nd moment at 1.6 K is $2.5(1)\mu_B$ aligned along the c axis. This magnetic structure is closely related to the low-temperature magnetic structure of the cubic parent compound $NdIn_3$.

DOI: 10.1103/PhysRevB.66.132417 PACS number(s): 75.25.+z, 75.30.Gw, 75.40.Cx

$NdRhIn_5$ crystallizes in the tetragonal $HoCoGa_5$ structure (space group $P4/mmm$),[1] and belongs to a large structural family of compounds with the chemical composition R_mMIn_{3m+2}, with $R=$ rare earth, $M=$ transition metal, and $m=1,2$. The tetragonal crystal structures of these compounds may be seen as m layers of RIn_3 and a layer of MIn_2 alternately stacked along the c axis. Included in this family are three newly discovered heavy-Fermion superconductors that have received considerable attention.[2–4] For example, $CeRhIn_5$, an antiferromagnet below $T_N=3.8$ K, undergoes a transition to a superconducting state at approximately 16 kbar with $T_C=2.1$ K.[2,5] Another member, $CeCoIn_5$ is an ambient pressure superconductor with a record setting $T_c=2.3$ K for heavy-Fermion superconductors.[4] Thermodynamic and transport measurements are indicative of unconventional superconductivity in which there may be line nodes in the superconducting gap.[6,7]

It is widely held that magnetic ground states of heavy-Fermion compounds are determined by the balance between competing Kondo and Ruderman-Kittel-Kasuya-Yosida (RKKY) interactions.[8] For f-electron magnetic materials, anisotropy is also known to affect the magnetic state.[9] Therefore studies of structurally related non-Kondo magnetic materials such as $NdRhIn_5$ may give insight into the evolution of magnetic properties in these materials.[10] For the present study, we have performed both powder and single-crystal neutron diffraction in order to determine the magnetic structure of the antiferromagnet $NdRhIn_5$. The results are compared to those of cubic $NdIn_3$, which may be considered the parent compound in the Nd_mMIn_{3m+2} series. Further comparisons are also made with the evolution of magnetic structures in the Ce-based series.

Single crystals of $NdRhIn_5$ were grown from an In flux. The lattice parameters are $a=4.630$ Å and $c=7.502$ Å at room temperature.[10] Neutron-diffraction experiments were performed at Chalk River Laboratories using the C-2 High Resolution Powder Diffractometer and the C-5 triple axis spectrometer in a two axis mode. Incident neutrons of wavelength 1.33 Å were selected using a Si monochromator for C-2, while 1.53-Å neutrons were selected with a Ge monochromator for C-5. In both cases, the sample temperature was regulated by a top loading pumped He cryostat.

In order to determine the magnetic propagation vector, powder-diffraction patterns were collected above and below the ordering temperature using C-2. The low-temperature pattern clearly shows additional magnetic reflections which can be indexed using a magnetic structure with the propagation vector $\mathbf{q}_M=(\frac{1}{2}0\frac{1}{2})$. This corresponds to a magnetic unit cell that doubles the chemical unit cell along the tetragonal a and c axes and contains four magnetic Nd ions.

Subsequently, a rectangular platelike sample of dimensions $\sim 3\times 3\times 0.7$ mm^3 with the (001) plane the largest surface was measured on C-5. The sample was mounted with the [010] direction vertical in order to access reciprocal-lattice points of the type $(h0l)$.

We observed temperature-dependent magnetic Bragg reflections at $(m/2,0,n/2)$, where m and n are odd integers, confirming the propagation vector found in powder diffraction. A typical elastic rocking scan taken at 1.6 K is shown in Fig. 1(a). The intensity of the $(\frac{3}{2}0\frac{1}{2})$ peak is shown in Fig. 1(b) as the square of the order parameter of the antiferromagnetic transition. The Néel temperature was determined to be 11.0(1) K, in good agreement with T_N found in specific-heat measurements.[10] The integrated intensities of magnetic Bragg reflections from such rocking scans were normalized to the (400) and (004) nuclear peaks to yield magnetic cross sections $\sigma_{obs}(\mathbf{q})=I(\mathbf{q})\sin(2\theta)$ in absolute units. The propagation vector $\mathbf{q}_M$ suggests a model in which Nd moments are aligned antiparallel in the [100] and [001] directions, and parallel in the [010] direction, resulting in the magnetic cross section[11]

$$\sigma(\mathbf{q})=\left(\frac{\gamma r_0}{2}\right)^2\langle m\rangle^2|f(q)|^2\langle 1-(\hat{\mathbf{q}}\cdot\hat{\mathbf{m}})^2\rangle, \qquad (1)$$

where $\gamma r_0/2=0.2695\times 10^{-12}$ cm/μ_B is the scattering length associated with $1\mu_B$, $\langle m\rangle$ is the staggered moment of the Nd ion, and $f(q)$ is the Nd^{3+} magnetic form factor.[12] The polarization factor $\langle 1-(\hat{\mathbf{q}}\cdot\hat{\mathbf{m}})^2\rangle$, averaged over possible magnetic domains with the assumption of equal occupation of the domains, is

$$\langle 1-(\hat{\mathbf{q}}\cdot\hat{\mathbf{m}})^2\rangle=1-\frac{\sin^2\alpha\sin^2\beta+2\cos^2\alpha\cos^2\beta}{2}, \qquad (2)$$

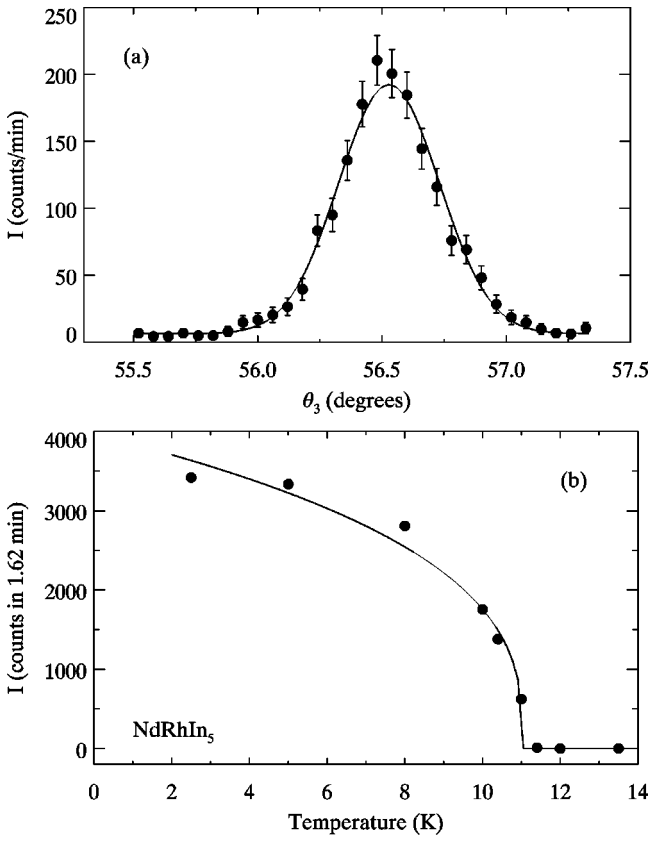

FIG. 1. (a) Elastic rocking scan through magnetic Bragg point $(\frac{1}{2}0\frac{5}{2})$ at 1.6 K. (b) Intensity of $(\frac{3}{2}0\frac{1}{2})$ reflection as a function of temperature. The Néel temperature is 11 K. The solid line is a guide for the eye.

where α is the angle between $\mathbf{q}$ and the c axis, and β is the angle between the magnetic moment and the c axis. The best least-squares fit to Eqs. (1) and (2) gives, within one standard deviation, $\beta=0$, which corresponds to magnetic moments aligned along the c axis, and reduces Eq. (1) to

$$\sigma(\mathbf{q})=\left(\frac{\gamma r_0}{2}\right)^2\langle m\rangle^2|f(q)|^2(1-\cos^2\alpha). \tag{3}$$

The best least squares fit of the experimental data was achieved using the spin-only Nd^{3+} form factor. Such a fit results in a staggered Nd moment at 1.6 K of $\langle m\rangle = 2.61(1)\mu_B$. Figure 2 shows the quantity $\sigma(q)/[(\gamma r_0/2)^2\langle m\rangle^2(1-\cos^2\alpha)]$, which is equal to the square of the magnetic form factor, $|f|^2$ [refer to Eq. (3)]. The solid line in Fig. 2 is the theoretical spin-only Nd^{3+} form factor.[12]

The high-temperature effective moment of $3.66\mu_B$, deduced from susceptibility data above 150 K, is in good agreement with the Hund's rule value of $3.62\mu_B$, indicating well localized Nd moments at high temperatures.[10] One thus expects some orbital contribution to the magnetic moment. The lower staggered moment of $2.61\mu_B$ found here, at 1.6 K, reflects the presence of crystalline electric field (CEF) effects.[9] We performed additional least-squares fits of the data using the orbit-only and spin+orbit form factors,[12] represented by the dotted and dashed lines in Fig. 2, respectively. Note that the data points in Fig. 2 were normalized to $\langle m\rangle = 2.61\mu_B$, determined with the spin-only form factor. On this scale, the best fits of the orbit-only and spin+orbit form factors intersect the vertical axis, at $|\mathbf{q}|=0$, at lower values. Since by definition, $|f(\mathbf{q}=0)|^2=1$, the dotted and dashed lines in Fig. 2 indicate that these fits result in lower Nd moments. For instance, using the spin+orbit form factor gives a staggered moment of $2.39(1)\mu_B$ and using the orbit-only form factor results in a staggered moment of $2.50(1)\mu_B$. Unfortunately, our experiment cannot determine exactly the orbital contribution to the magnetic moment. Therefore we take the results of the fits using the spin-only (solid line) and spin+orbit (dashed line) form factors to be the upper and lower bounds to the staggered moment, respectively. This yields a staggered moment of about $2.5(1)\mu_B$ per Nd.

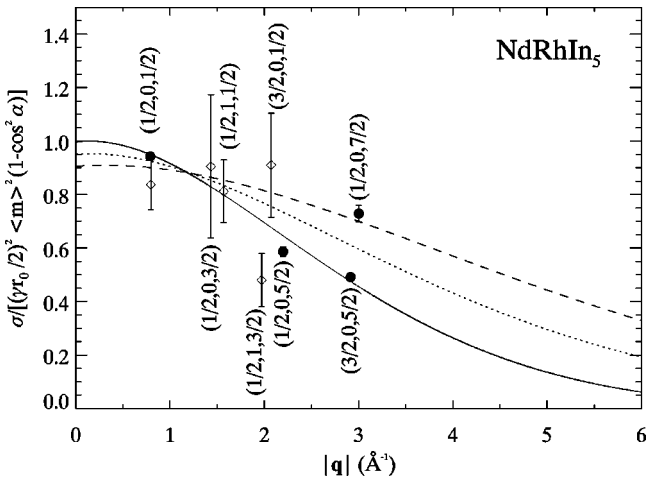

FIG. 2. The q dependence of the square of the magnetic form factor, $|f|^2$ as given by the quantity, $\sigma(q)/[(\gamma r_0/2)^2\langle m\rangle^2(1-\cos^2\alpha)]$ [refer to Eq. (3)]. Single-crystal data are shown as solid circles, while data from the powder-diffraction experiment are represented by open diamonds. The value of the staggered Nd moment, $\langle m\rangle = 2.61\mu_B$ was taken from the best least-squares fit of the data, which was achieved using the spin-only Nd^{3+} form factor. The solid line is the theoretical spin-only Nd^{3+} form factor. Analysis using the orbit-only form factor resulted in a lower staggered moment of $2.50(1)\mu_B$. Since the data have been normalized to $\langle m\rangle = 2.61\mu_B$, determined with the spin-only form factor, the dotted line, which represents the orbit-only form factor, has a lower intercept on this scale, reflecting a lower staggered moment. Similarly, the spin+orbit form factor (dashed line) also resulted in a smaller moment of $2.39(1)\mu_B$. All Nd^{3+} form factors were taken from Ref. 12.

Now, we compare the magnetic structure of $NdRhIn_5$ with that of its cubic parent compound $NdIn_3$, which orders antiferromagnetically below $T_N=6$ K and exhibits a complex magnetic phase diagram, including two additional antiferromagnetic transitions at 4.61 and 5.13 K.[13–15] The two intermediate phases were determined to have incommensurate structures with magnetic propagation vectors $\mathbf{q}_M = (\frac{1}{2}0.037\frac{1}{2})$ and $(\frac{1}{2}0.017\frac{1}{2})$, respectively, while the ground-state structure was determined to be commensurate with $\mathbf{q}_M=(\frac{1}{2}0\frac{1}{2})$ and staggered Nd moments of approximately $2.0\mu_B$ with [010] the easy magnetization direction.[16,17] The

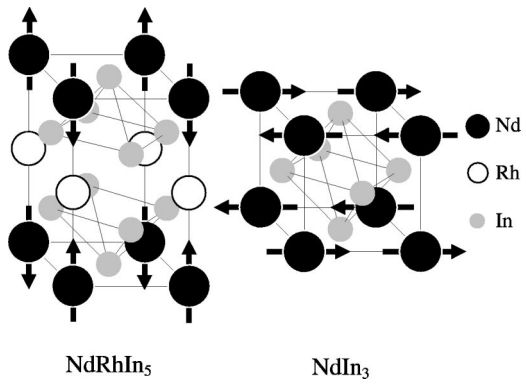

FIG. 3. Schematic representation of the crystallographic and magnetic structure of $NdRhIn_5$ in a chemical unit cell. The commensurate magnetic structure of $NdIn_3$ below 4.6 K from Ref. 17 is also shown for comparison. The arrows indicate the directions of the Nd moments.

complexity of the magnetic phase diagram of $NdIn_3$ was also verified by various field-induced transitions in the H-T phase diagram.[16,17] A model including competing CEF and magnetic exchange anisotropies has satisfactorily described the complex phase diagrams of $NdIn_3$.[17]

The magnetic structure of $NdRhIn_5$ is shown together with that of $NdIn_3$ below 4.6 K in Fig. 3. In comparison to $NdIn_3$, the moment direction relative to the magnetic wave vector is rotated by 90° in $NdRhIn_5$. However, the phases among the magnetic moments are identical in both cases.

For the tetragonal $NdRhIn_5$, the insertion of a $RhIn_2$ layer nearly doubles the Néel temperature of $NdIn_3$. No evidence of additional transitions below T_N was observed in our study as well as in bulk measurements down to 1 K.[10] In addition, field-dependent heat capacity revealed no evidence for field-induced transitions up to $H=9$ T applied in the ab plane and one transition at about 7 T for $H\|c$ axis.[18] Therefore, although the magnetic structure of $NdRhIn_5$ is closely related to the parent compound $NdIn_3$, the relatively simple H-T phase diagram of $NdRhIn_5$ suggests that the commensurate antiferromagnetic structure $\mathbf{q_M}=(\frac{1}{2}0\frac{1}{2})$ is more robust and stable in the tetragonal variant. In fact, the Nd^{3+} ($J=9/2$) ion in axial symmetry commonly has its multiplet split in anisotropic doublets (with g value $g_{\|c}\gg g_{\perp}$) favoring the Nd spins to point along the c axis which is consistent with our results. Therefore the tetragonal symmetry may produce an improved matching among the existing CEF, magnetocrystalline and exchange coupling anisotropies for $NdRhIn_5$.

We now extend our discussion to the Ce-based series. For $CeRhIn_5$, the nearest-neighbor antiferromagnetic structure of the parent compound $CeIn_3$ is maintained within the $CeIn_3$ layers. However, the magnetic moments in $CeRhIn_5$ form an incommensurate spiral along the c axis.[19,20] Furthermore, T_N is reduced by a factor of 2 for $CeRhIn_5$ ($T_N\sim 4$ K) compared to $CeIn_3$ ($T_N\sim 10$ K), which is just the opposite of the situation in $NdRhIn_5$ and $NdIn_3$.

These contrary behaviors may be understood by noticing that the magnetic moments in $CeRhIn_5$ lie in the ab plane,[19] whereas the CEF anisotropy tends to favor energetically the Ce spins to point along the c axis.[2,21] Therefore there might be in $CeRhIn_5$ competing anisotropic magnetic interactions that lead to an incommensurate magnetic state at lower T_N when compared to $CeIn_3$. Accordingly, field-dependent heat capacity[22] has revealed a rich H-T phase diagram with field-induced transitions similar to what was observed in $NdIn_3$, where competing CEF and exchange interaction anisotropies were considered.

Alternatively, antiferromagnetic correlations across the intervening $RhIn_2$ layers in $NdRhIn_5$ are in some sense more reminiscent of Ce_2RhIn_8, in which the magnetic structure within $CeIn_3$ bilayers are unmodified relative to cubic $CeIn_3$ and the correlations across the $RhIn_2$ layers are antiferromagnetic.[23]

In conclusion, we find a commensurate antiferromagnetic structure, as represented in Fig. 3, with $\mathbf{q}_M=(\frac{1}{2}0\frac{1}{2})$ for $NdRhIn_5$. The staggered Nd moment is determined at 1.6 K to be $2.5(1)\mu_B$ aligned along the tetragonal c axis. The phases of the nearest-neighbor Nd atoms are the same as in the commensurate phase of cubic $NdIn_3$.

Work at Los Alamos was performed under the auspices of the U.S. Department of Energy. H.N. acknowledges support from the NSF (grant number DMR-0094241).

*Electronic address: schang@nmsu.edu

[1] Y. N. Grin, Y. P. Yarmolyuk, and E. I. Giadyshevskii, Sov. Phys. Crystallogr. **24**, 137 (1979).
[2] H. Hegger, C. Petrovic, E. G. Moshopoulou, M. F. Hundley, J. L. Sarrao, Z. Fisk, and J. D. Thompson, Phys. Rev. Lett. **84**, 4986 (2000).
[3] C. Petrovic, P. G. Pagliuso, M. F. Hundley, R. Movshovich, J. L. Sarrao, J. D. Thompson, Z. Fisk, and P. Monthoux, J. Phys.: Condens. Matter **13**, L337 (2001).
[4] C. Petrovic, R. Movshovich, M. Jaime, P. G. Pagliuso, M. F. Hundley, J. L. Sarrao, Z. Fisk, and J. D. Thompson, Europhys. Lett. **53**, 254 (2001).
[5] S. Kawasaki, T. Mito, G. Q. Zheng, C. Thessieu, Y. Kawasaki, K. Ishida, Y. Kitaoka, T. Muramatsu, T. C. Kobayashi, and D. Aoki, Phys. Rev. B **65**, 020504 (2001).
[6] R. Movshovich, M. Jaime, J. D. Thompson, C. Petrovic, Z. Fisk, P. G. Pagliuso, and J. L. Sarrao, Phys. Rev. Lett. **86**, 5152 (2001).
[7] K. Izawa, H. Yamaguchi, Y. Matsuda, H. Shishido, R. Settai, and Y. Ōnuki, Phys. Rev. B **87**, 057002 (2001).
[8] S. Doniach, in *Valence Instabilites and Related Narrow Band Phenomena*, edited by R. D. Parks (Plenum, New York, 1977).
[9] J. Jensen and A. R. Mackintosh, *Rare Earth Magnetism: Structures and Excitations* (Oxford University Press, Oxford, 1991).
[10] P. G. Pagliuso, J. D. Thompson, M. F. Hundley, and J. L. Sarrao, Phys. Rev. B **62**, 12 266 (2000).
[11] G. L. Squires, *Introduction to the Theory of Thermal Neutron Scattering* (Cambridge University Press, Cambridge, 1978).
[12] M. Blume, A. J. Freeman, and R. E. Watson, J. Chem. Phys. **37**, 1245 (1962).
[13] K. H. J. Buschow, H. W. D. Wijn, and A. M. V. Diepen, J. Chem. Phys. **50**, 137 (1969).

[14] A. Czopnik, N. Iliew, B. Stalinski, C. Bazan, H. Madge, and R. Pott, Physica B **130**, 259 (1985).
[15] A. Czopnik, J. Kowalewski, and M. Hackemer, Phys. Status Solidi A **127**, 243 (1991).
[16] S. Mitsuda, P. M. Gehring, G. Shirane, H. Yoshizawa, and Y. Ǫnuki, J. Phys. Soc. Jpn. **61**, 1469 (1992).
[17] M. Amara, R. M. Galéra, P. Morin, T. Veres, and P. Burlet, J. Magn. Magn. Mater. **130**, 127 (1994); M. Amara, R. M. Galéra, P. Morin, J. Voiron, and P. Burlet, *ibid.* **131**, 402 (1994); **140-144**, 1157 (1994).
[18] P. G. Pagliuso *et al.* (private communication).
[19] W. Bao, P. G. Pagliuso, J. L. Sarrao, J. D. Thompson, Z. Fisk, J. W. Lynn, and R. W. Erwin, Phys. Rev. B **62**, R14 621 (2000); **63**, 219901(E) (2001).
[20] N. J. Curro, P. C. Hammel, P. G. Pagliuso, J. L. Sarrao, J. D. Thompson, and Z. Fisk, Phys. Rev. B **62**, R6100 (2000).
[21] P. G. Pagliuso, N. J. Curro, N. O. Moreno, M. F. Hundley, J. D. Thompson, J. L. Sarrao, and Z. Fisk, Physica B **320**, 370 (2002).
[22] A. L. Cornelius, P. G. Pagliuso, M. F. Hundley, and J. L. Sarrao, Phys. Rev. B **64**, 144411 (2001).
[23] W. Bao, P. G. Pagliuso, J. L. Sarrao, J. D. Thompson, Z. Fisk, and J. W. Lynn, Phys. Rev. B **64**, 020401 (2001).